

# Electrowetting-on-dielectric Induced Droplet Actuation in M×N Array of Electrode

Shiraz Sohail<sup>\*1</sup>, Debanjan Das<sup>1</sup>, Soumen Das<sup>2</sup>, Karabi Biswas<sup>1</sup>

<sup>1</sup>Electrical Engineering Department, IIT Kharagpur

<sup>2</sup>School of Medical Science and Technology, IIT Kharagpur

\*Electrical Engineering Department, IIT Kharagpur, pin-721302, Kharagpur, [ssohail@iitkgp.ac.in](mailto:ssohail@iitkgp.ac.in)

**Abstract:** One of the major challenges in EWOD device is to address each electrode individually in  $M \times N$  array of electrode using simple fabrication architecture without compromising in system performance. Cross-reference scheme, which allows single-layer electrode fabrication for 2D droplet movement consist of both top and bottom substrate each consist of orthogonally aligned parallel electrode assembly in the XY-plane. The present work focuses on simulation of driving force in the cross-reference design using 3D voltage distribution plots obtained through AC-DC module of COMSOL Multiphysics software. The cross-reference scheme is not only easy to fabricate but also does not compromise with system performance as in the case of classical scheme due to large electrode gap. For simulation, a 3 x 3 array of electrode has been considered for 2D droplet motion by actuating inner electrodes. Voltage distribution across different layers has been calculated from field distribution plot and used in energy based model for estimating actuation force during droplet transition.

**Keywords:** Electrowetting, COMSOL,  $M \times N$  array, electrode addressing.

## 1. Introduction

Droplet-based microfluidics (Digital microfluidics) is a new and emerging trend in microelectrofluidic systems (MEFS) and micro-total analysis systems ( $\mu$ TAS) in the past decade that involves manipulation of discrete fluid micropackets of controlled volume and composition in micro and nano channels [1][2]. In this, multiple droplets are used like small microreactors. Multiple experiments can be performed on a single chip surface by modifying the control software through multiplexing as each droplet is spatially confined. These devices are highly scalable and reconfigurable, and capable of performing high throughput analysis with efficient control. Their reconfigurability reduces cost, weight and analysis time [1].

Electrowetting-on-dielectric (EWOD) is arguably the most flexible and powerful tool, used in many LOC platforms because there is no need for a closed channel network and external pump to manipulate the droplets or mechanical parts to move or guide the droplets [2][3][4][5][6].

In EWOD-based devices, independent addressing of each electrode is required for transport of multiple droplets in multiple tracks simultaneously by modifying the control software through multiplexing. Independent addressing of each electrode has been demonstrated by several research groups in 1D motion for specific task in simple MEFS. But the potential use of reconfigurability in complex MEFS based on EWOD technology demands 2D motion of droplets and requires a two dimensional matrix of electrode system.

Electrically addressing of inner electrodes independently in 2D matrix of order 3x3 or greater by single level metallization are carried out traditionally by running conduction lines between the electrode gaps. The conduction lines leads to unwanted wetting of non electrode area and seriously affects the droplet track especially when many conduction lines are routed between electrode gaps [7]. Furthermore, as the order of 2D matrix system increases, the number of conduction lines from the inner electrodes to the external control circuit increases likewise. These access lines must run through the electrode gaps, which should be minimized in order to maintain the driving efficiency of EWOD technology [7][8].

Multi level metallization technique using typical integrated circuit (IC) fabrication methods on glass or Si substrates has been used to avoid parasitic unwanted wetting effect through underlying conduction lines (i.e. by burying conduction lines beneath the electrode assembly layer). Gascoyne et al. 2004 [9] demonstrated a  $32 \times 32$  DEP programmable fluidic process chip using CMOS architecture on a silicon-on-insulator (SOI) IC chip. While Li et al. 2008 [7] has demonstrated a multi-level

metallization EWOD array with low fabrication temperature to develop high-k tantalum pentaoxide insulating layer compatible with CMOS fabrication procedure for reducing voltage requirement. Multi-level metallization EWOD array offers several benefits such as integration of sensing (e.g. pH, temperature, position, light, voltage etc) and controlling (e.g. temperature control) electrodes, less number of bond pads, simple packaging etc. However due to multiple thin-film deposition, lithography, patterning and planarization, fabrication cost becomes high and process steps also become lengthy and complex [7][8].

Gong et al. 2005 &2008 [10][8] and Paik et al. 2006 [11] have demonstrated a low cost and flexible packaging scheme by using printed circuit board (PCB) technology together with land grid array (LGA) sockets in which multilayer electrical access lines were created through hole contacts that allow high density contacts to be made on the back side of the substrate. However, due to surface roughness and resistance against droplet movement in case of Gong et al 2008 and thick soldermask insulator in case of Paik et al. 2006, the actuation voltage achieved was high (Gong et al 2008 ~500 V; Paik et al. 2006 ~ 130V). Since the glass transition temperature of FR4 (the polymer used as PCB substrate material) is 185 °C, PCBs cannot be subjected to high temperature processes for depositing high-k dielectric material as insulator such as plasma-enhanced chemical vapor deposition (PECVD) [8]. In addition , this scheme too is limited to the practical aspect of the interconnect since a 32x32 digital microfluidic array [9] used in requires over 1000 pins [7].

Fan et al. 2003 [12] reported the concept of cross-reference driving, which allows single-layer electrode fabrication for 2D droplet movement. The present work focuses simulation of driving force in the cross-reference design using 3D voltage distribution plots obtained through AC-DC module of COMSOL Multiphysics software. The cross reference design consists of both top and bottom substrate each consist of orthogonally aligned parallel electrode assembly in the XY-plane for 2D droplet motion in an  $M \times N$  matrix of electrode assembly as shown in Figure 3. By energizing the row and column electrodes with opposite signals, the electrode spots at their intersection

become most hydrophilic and thus the droplet moves toward them. Electrodes require to actuate for droplet movement to a specific electrode is given by its Cartesian coordinates (X-top, Y-bottom) keeping all other electrodes at the ground potential. The proposed scheme is not only easy to fabricate but also does not compromise system performance as in the case of classical scheme due to large electrode gap. For simulation, a  $3 \times 3$  array of electrode has been considered for 2D droplet motion by actuating inner electrodes. Voltage distribution across different layers has been calculated from field distribution plot and used in energy based model [13] [3] for estimating actuation force during droplet transition.

The paper is structured as follows. Section 2 introduces the theory and energy based model for calculating driving force during droplet transition. Use of COMSOL Multiphysics has been presented in Section 3. Result and discussion is presented in Section 4 and conclusion is in section 5.

## 2. Theory

EWOD system can be analyzed from energy-minimization considerations, according to which the droplet minimizes its surface energy by transiting to the actuated electrode. The energy gradient is thus the driving force behind EW-induced motion of a fluid element. In this work, an analytical energy-based model proposed by Bahadur 2006 [13] has been used to predict EWOD actuation force on a droplet during its transition.

A traditional covered two plate EWOD system used to move droplet from non-actuated electrode to actuated electrode and its electrical equivalent circuit has been shown in figure 1 and 2 respectively.

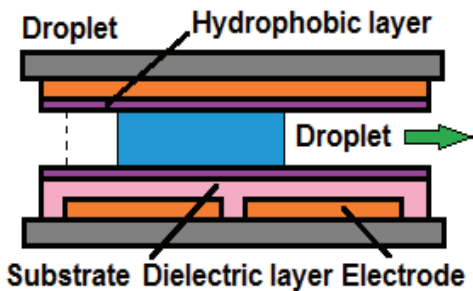


Figure 1: Schematic diagram of a droplet transition by electrowetting-on-dielectric.

This consists of bottom patterned control electrode assembly and top continuous electrode. Both, top and bottom electrodes are coated by a dielectric layer and a thin hydrophobic layer. There are three capacitors:  $C_1$  (between actuated electrode and droplet),  $C_2$  (between non-actuated electrode and droplet) and  $C_3$  (between droplet and top ground electrode) in the electrical circuit.

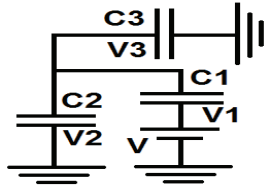


Figure 2: Electrical equivalent circuit of the typical two plate covered EWOD system

The capacitance of these capacitors varies with droplet leading edge  $x$  as it varies from 0 to  $L$  (pitch length) during transition. The actuation force can be modeled by analyzing the droplet energy as a function of the droplet leading edge  $x$ . The reduction in interfacial tension is caused by these three capacitors and can be obtained by analysis of capacitive network.

The droplet free energy can be expressed as the sum of all the interfacial energies:

$$E(x) = \gamma_{SL} \times A_1(x) + \gamma_{SL} \times A_2(x) + \gamma_{SL} \times A_3(x) + \gamma_{LA} \times A_{SIDE} \quad (1)$$

Here  $\gamma_{SL}$ ,  $\gamma_{LA}$  and  $A_{SIDE}$  represent solid–liquid interfacial energy, liquid–air interfacial energy and cylindrical side around the droplet. Lippmann equation [14] is used to quantify the decrease in solid–liquid interfacial energy upon the application voltage  $V$  is given by:

$$\gamma_{SL}^V = \gamma_{SL}^0 - \frac{k\epsilon_0 V^2}{2t} \quad (2)$$

Applying Lippmann equation to (2) assuming liquid–air interfacial energy remain unchanged [15], the droplet free energy can be expressed as:

$$E(x) = \left( \gamma_{SL}^0 - \frac{k\epsilon_0 V_1^2}{2t} \right) \times A_1(x) + \left( \gamma_{SL}^0 - \frac{k\epsilon_0 V_2^2}{2t} \right) \times A_2(x) + \left( \gamma_{SL}^0 - \frac{k\epsilon_0 V_3^2}{2t} \right) \times A_3(x) + \gamma_{LA} \times A_{SIDE} \quad (3)$$

The negative derivative of the Energy variation gives the electrical actuation force on the droplet as a function of the transition position  $x$ . The actuation force has three components corresponding to the three regions of the droplet surface which undergo interfacial energy change under the influence of the applied voltage. Results obtained from this model are identical to purely electromechanical model [13].

The cross-reference design for  $3 \times 3$  2D matrix electrode system for addressing inner electrode has been shown in figure 3. This matrix can easily be represented by Cartesian coordinate system by assigning top plate as X and bottom plate as Y.

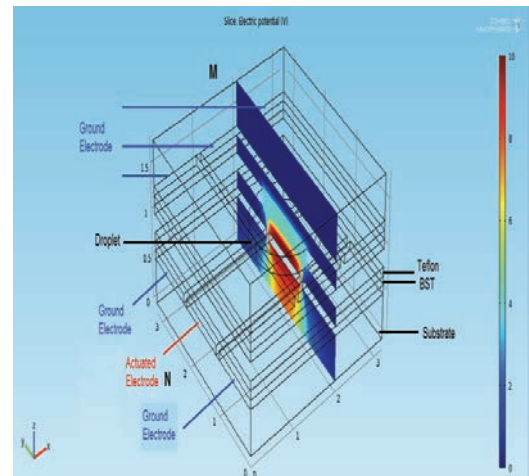


Figure 3: Cross reference scheme for single-layer electrode fabrication for 2D droplet movement.

Consider initially the droplet is placed at the center electrode 2, 2 (i.e. X-2, Y-2). Now to address this electrode, the second electrode from top or second electrode from bottom will be actuated depending upon direction of motion (i.e. X or Y). The droplet can be moved in both X and Y-direction. For example, to move the droplet in X-direction, it can either be moved to 1, 2 or 3, 2. Similarly it can be moved to 2, 1 or 2, 3 to move in the Y-direction. Considering the droplet has to be moved to 1, 2 for the movement in X-direction. So, first electrode from top will be energized. This state of the device can be represented by the electrical equivalent circuit as shown in figure 2. In this case capacitance is represented by  $C_1$  between first top electrode and

droplet,  $C_2$  top electrode and droplet and  $C_3$  droplet and second bottom electrode. Similarly if the droplet is moved to 2, 1 in Y-direction by energizing first electrode from bottom, capacitance is represented by  $C_1$  between droplet and first bottom electrode,  $C_2$  between droplet and second bottom electrode and  $C_3$  between second top electrode and droplet. So it is seen here that in the cross reference design also there only three capacitors in the electrical equivalent circuit and actuation force can directly be computed from equation 3. When droplet is actuated in different direction,  $c_1$ ,  $c_2$  and  $c_3$  represent different capacitor. But there variations are symmetrical in both directions and finally lead to same force pattern whether moved in X-direction or Y.

### 3. Use of COMSOL

COMSOL Multiphysics software has been used to calculate the voltage drop  $V_1$ ,  $V_2$  and  $V_3$  across capacitor  $C_1$ ,  $C_2$  and  $C_3$  respectively as shown in figure 2. Cross reference design of  $3 \times 3$  EWOD system has been analyzed using AC-DC module tool box of which schematic set-up has been shown in figure 3. Voltage drop across capacitors have been calculated by first chopping the droplet and electrode assembly atop of which droplet transition has to take place by a 2D ZX-plane. Considering the droplet initially sits atop 2, 2 electrode and by actuating first electrode in top substrate, it has to move to 1, 2 in X-direction. So in this case, it has been taken at  $Y=1.6$  mm. Thereafter, two vertical 2D lines have been drawn on the XZ-plane, one on actuated electrode (point 1:  $X=0$ ,  $Y=1.15$  and point 2:  $X=1.8$ ,  $Y=1.15$  mm) and other at unactuated electrode (point 1:  $X=0$ ,  $Y=0.95$  and point 2:  $X=1.8$ ,  $Y=0.95$  mm). Voltage distribution across these lines has been drawn by 1D plot and exported to MATLAB to calculate potential difference (p.d.) across these capacitors. Four points have been chosen to calculate p.d. across capacitors from the 1D plot. These points are as follow: 0.6, 0.8, 1.0 and 1.2. These points are the interface point between metal electrode and insulation layer (bottom side), insulation layer and droplet (bottom side), droplet and insulation layer (top side) and insulation layer and metal electrode (top side) along the height (Z-axis) of the device respectively.

The droplet has been shifted from unactuated plate to the actuated plate in step of 0.1mm along X-axis starting from  $x=1.6$  to 0.5 mm for complete transition. For each step, 1D plot of vertical lines has been exported to MATLAB. In this way, three vectors of  $V_1$ ,  $V_2$  and  $V_3$  have been obtained for each step transition of droplet. Finally these vectors have been used in the MATLAB program to calculate the actuation force during complete transition of the droplet. In AC-DC simulation, TERMINAL boundary condition (10V) has been applied to all the faces of the actuated electrodes while all the face of unactuated electrode has been assigned GROUND boundary condition.

### 4. Result and discussion

For simulation, a  $3 \times 3$  array of electrode has been considered for 2D droplet motion by actuating inner electrodes as shown in figure 3. The top substrate consists of three electrode of length 3.2 mm, width 1mm and depth 0.1mm aligned parallel to X-axis. The gap between electrodes has been kept 0.1mm. Similarly, bottom substrate too consists of three electrodes of same dimension but aligned parallel to Y-axis. By energizing the row or column electrodes with opposite signals, the electrode spots at their intersection become most hydrophilic and thus the droplet moves toward them. Here, the intersection area between top and bottom electrode is  $1 \times 1$  mm. For moving droplet in X-direction, top electrode has to be activated alternately while for moving in Y-direction bottom electrodes. Two layers of thin film, one of which is made of very high dielectric constant and other made of hydrophobic material, is the current trend in order to reduce the required actuation voltage for transition. So in simulation, both top and bottom set of electrodes are considered to be coated with BST film ( $\epsilon_r=180$ , thickness-0.1 mm) and Teflon film ( $\epsilon_r=2.1$ , thickness-0.1 mm) as dielectric and hydrophobic layer respectively.

The droplet has been considered to be circular shape of diameter  $L$  (i.e.  $2r=L$ ) and assumed to move as a rigid body, maintaining its circular shape during the transition. When a droplet moves from one electrode to the other, voltage distribution changes across all the three capacitors as shown in figure 4.

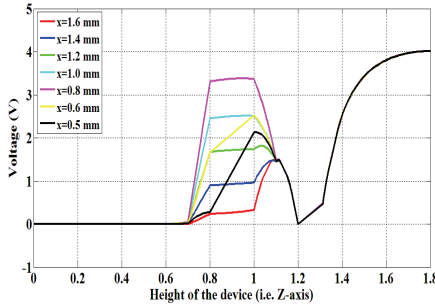


Figure 4: Voltage distribution along the height of the device (Z-axis) at  $x=0.5$  to  $1.6$  mm.

The circular area in contact of the droplet can be divided into two parts at a particular position ( $x$ ), one part comes under the actuated electrode while the other comes under unactuated electrode. These two parts have different potential but there is very small variation of potential in these two parts individually. This can be seen from the XY cut plane at  $Z=1.05$  mm as shown in figure 5.

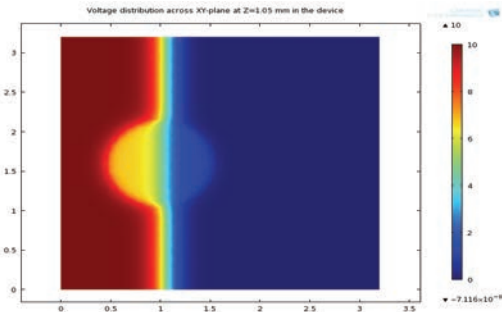


Figure 5: Voltage distribution across XY-plane at  $Z=1.05$  mm when  $x=1.0$  in the EWOD device.

Similar observations have been found for  $x$  varies from 0.5 to 1.6 mm and also across XY-plane at  $Z=0.8$  mm. From these observations, it was decided to take 1D plot of two vertical 2D lines on XZ-plane, one on actuated electrode and other at unactuated electrode to calculate voltage.

The voltage distribution 1D plot of the vertical 2D lines has been used to calculate three vectors  $V_1$ ,  $V_2$  and  $V_3$  of the p.d across capacitors  $C_1$ ,  $C_2$  and  $C_3$  for  $x=1.6$  to  $0.5$  mm in step of  $0.1$  mm. Thereafter, these vectors have been applied to equation 3 to calculate actuation force during complete transition from one plate to the other through MATLAB program as shown in figure 6. The actuation force  $F(x)$  has three components  $F_1(x)$ ,  $F_2(x)$  and  $F_3(x)$  corresponding

to the three capacitors  $C_1$ ,  $C_2$  and  $C_3$  respectively responsible for interfacial energy change under the influence of the applied voltage.

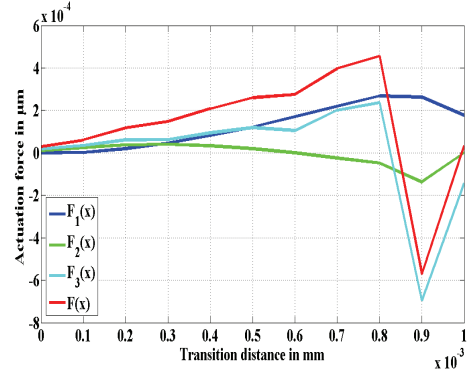


Figure 6: Actuation force during droplet transition from electrode to the other.

It is seen that the total force is positive up to  $x=0.8$  mm, and it has positive slope as well. But beyond  $x=0.8$  mm, the slope and magnitude of resultant the force  $F(x)$  becomes negative and can be attributed as braking action to the droplet inertial moment. Because of which the droplet finally stops to the actuated electrode and don't move beyond that.  $F_3(x)$  is responsible for the negative slope of  $F(x)$  beyond  $x=0.8$ . At the end, undershoot in the  $F(x)$  is also responsible for oscillatory motion in droplet before coming to rest.

## 5. Conclusion

The cross reference scheme for addressing electrode in  $M \times N$  array is not only easy to fabricate but also does not compromise system performance as in the case of classical scheme due to large electrode gap. The cross reference scheme can easily adopt the Cartesian coordinate system to address an electrode and its equivalent electrical circuit remains same as two plate covered EWOD system. However, the simultaneous driving of multiple droplets in all possible combination in cross-referencing scheme is limited. The force calculation during transition of droplet using COMSOL Multiphysics gives better insight into EWOD dynamics without entrapping into long calculation to calculate voltage distribution vectors. It also explains braking action and oscillatory motion in the droplet before coming to rest.

## 6. Reference

- [1] A. Ahmadi, K. D. Devlin, and M. Hoofifar, "Numerical study of the microdroplet actuation switching frequency in digital microfluidic biochips," *Microfluidics and Nanofluidics*, pp. 1-11, Aug. 2011.
- [2] N. Vergauwe et al., "Controlling droplet size variability of a digital lab-on-a-chip for improved bio-assay performance," *Microfluidics and Nanofluidics*, vol. 11, no. 1, pp. 25-34, Jan. 2011.
- [3] R. Malk, Y. Fouillet, and L. Davoust, "Rotating flow within a droplet actuated with AC EWOD," *Sensors and Actuators B: Chemical*, vol. 154, no. 2, pp. 191-198, Jun. 2011.
- [4] S. K. Chung, K. Rhee, and S. K. Cho, "Bubble actuation by electrowetting-on-dielectric (EWOD) and its applications: A review," *International Journal of Precision Engineering and Manufacturing*, vol. 11, no. 6, pp. 991-1006, Dec. 2010.
- [5] M. J. J. Schertzer, P. E. Sullivan, and R. Ben-Mrad, "Using capacitance measurements in EWOD devices to identify fluid composition and control droplet mixing," *Sensors and Actuators B:*, vol. 145, no. 1, pp. 340-347, Mar. 2010.
- [6] F. Mugele, "Fundamental challenges in electrowetting: from equilibrium shapes to contact angle saturation and drop dynamics," *Soft Matter*, vol. 5, no. 18, p. 3377, 2009.
- [7] Y. Li et al., "Anodic Ta<sub>2</sub>O<sub>5</sub> for CMOS compatible low voltage electrowetting-on-dielectric device fabrication," *Solid-State Electronics*, vol. 52, no. 9, pp. 1382-1387, Sep. 2008.
- [8] J. Gong and C.-J. "CJ" C. Kim, "Direct-referencing Two dimensional array Digital Microfluidics Using Multi-layer Printed Circuit Board," *Journal of microelectromechanical systems*, vol. 17, no. 2, pp. 257-264, 2008.
- [9] P. R. C. Gascoyne et al., "Dielectrophoresis-based programmable fluidic processors," *Lab on a chip*, vol. 4, no. 4, pp. 299-309, Aug. 2004.
- [10] J. Gong and C.-J. "CJ" Kim, "Two-Dimensional digital microfluidic system by multi-layer printed circuit board," in *17th IEEE International Conference on Micro Electro Mechanical Systems; Maastricht, Netherlands*, 2005, pp. 355-358.
- [11] P. Paik, "Adaptive hot-spot cooling of integrated circuits using digital microfluidics," Duke University, 2006.
- [12] S.-K. Fan, C. Hashi, and C.-J. Kim, "Manipulation of multiple droplets on N×M grid by cross-reference EWOD driving scheme and pressure-contact packaging," in *IEEE The Sixteenth Annual International Conference on Micro Electro Mechanical Systems, 2003. MEMS-03 Kyoto*, 2003, pp. 694-697.
- [13] V. Bahadur and S. V. Garimella, "An energy based model for electrowetting induced droplet actuation," *Journal of Micromechanics and Microengineering*, vol. 16, no. 8, pp. 1494-1503, Aug. 2006.
- [14] J. Berthier, *Microdrops and digital microfluidics*. Norwich, NY, USA: William Andrew Publishing, 2008, p. 441.
- [15] F. Mugele and J.-C. Baret, "Electrowetting: from basics to applications," *Journal of Physics: Condensed Matter*, vol. 17, no. 28, p. R705-R774, Jul. 2005.